

## New Synthesis Method of Biopolymer Composites Based on Alginate, Carrageenan and ZnONPS for Wound Healing Applications

Ali Fahem Getran Khazaali<sup>1</sup>  , Mohammed Kassim. Al-Hussainawy<sup>\*2,5</sup>  , Makarim A. Mahdi<sup>3</sup>   Waleed K. Abdulsahib<sup>4</sup>   and Layth S. Jasim Al-Hayder<sup>3</sup>  

<sup>1</sup>Department of Pharmaceutical Chemistry, College of Pharmacy, University of Al-Qadisiyah, Al Diwaniyah, Iraq

<sup>2</sup>Ministry of Education, Directorate of Education Al-Muthanna, Al-Samawah, AL-Muthanna, Iraq.

<sup>3</sup> Department of Chemistry , College of Education, University of Al-Qadisiyah, Diwaniya , Iraq.

<sup>4</sup>Department of Pharmacology and Toxicology, College of Pharmacy, Al-Farahidi University, Baghdad, Iraq.

<sup>5</sup>National University of Science and Technology, Nasiriyah, Dhi Qar, Iraq.

\*Corresponding author

Received 29/3/2023, Accepted 9/11/2023, Published 20/12/2024



This work is licensed under a Creative Commons Attribution 4.0 International License.

### Abstract

Hydrogels, being a drug delivery system, have great significance, particularly for the topical application in the treatment of open wounds. Their non-adhesiveness, moisture retention, and exudate absorption properties make them ideal for wound healing applications. Using a novel synthesis method, the biomedical hydrogels carrageenan/alginate ( $\kappa$ C-Sa) and carrageenan/alginate/ZnO ( $\kappa$ C-Sa/ZnO) were synthesized through modified free radical polymerization with acrylic acid as a cross-linker. The hydrogels were characterized using FTIR, FE-SEM, EDX, TEM, and photographic images.  $\kappa$ C-Sa and  $\kappa$ C-Sa/ZnO were applied as wound healers for injured rats. The synthesized hydrogels have a microstructure, semicrystalline properties, and good ZnO distribution for  $\kappa$ C-Sa/ZnO; ZnONPs added to the polymer matrix increased the swelling ratio to 800%. while the water loss percent for  $\kappa$ C-Sa is 76% more than  $\kappa$ C-Sa/ZnO (70%) in 25 h at room temperature. The hydrogel of  $\kappa$ C-Sa/ZnO shows more an antibiotic activity than  $\kappa$ C-Sa. The hydrogels were biocompatible when evaluated for their cytotoxic effect using the fibroblast cell line of mice (L929), where  $\kappa$ C-Sa/ZnO was more biocompatible than  $\kappa$ C-Sa. The  $\kappa$ C-Sa/ZnO hydrogel provided more healing than the  $\kappa$ C-Sa at 14 days, and this was diagnosed by histological analysis. **Keywords:** Antibacterial, Alginate-Carrageenan, Composites, Cytotoxicity, Hydrogel, Wound Dressing, ZnO nanoparticles.

### Introduction

The process of regenerating new cells and tissues to repair damaged structures during wound healing is exceedingly complicated and dynamic, involving a series of molecular, physiological, and biochemical processes. The selection of the proper wound dressing material is crucial for wound management. Ideal wound dressings should suppress scar formation, maintain skin homeostasis, reduce microbial invasion, hasten wound healing through epithelialization, and be cost-effective<sup>(1)</sup>. Investigations have recently focused on the creation of biopolymer-based platforms due to their helpful properties, which could be a substantial advantage in biomedical and wound healing applications<sup>(2)</sup>. Biopolymers contain several active groups such as hydroxyls, carboxylic acids, sulfates, and minerals, which are among the active constituents in hydrogels<sup>(3)</sup>. Biopolymer has traditionally been used to treat burns, open sores that won't heal, and infected sores or ulcers. Nanoporous gel structures known as hydrogels are three-dimensional (3D)

hydrophilic polymers that can be used for a variety of purposes, including tissue engineering, food additives, wound dressing, cell encapsulation, and drug administration<sup>(4)</sup>. Hydrogels are created by crosslinking gel precursors. Additionally, hydrogel-based structures have mostly been utilized for the delivery of medications. This is due to its special properties, which include a lot of water, smoothness, elasticity, and the ability to generate damp surroundings that prevent the injury from becoming dry<sup>(5,6)</sup>. The top biomedical platforms for treating different kinds of wounds when it comes to hydrogels are those in their natural forms. Polymers' enhanced pharmacokinetic properties have made them a crucial component of medication delivery systems. Since they circulate more quickly than traditional tiny medication molecules, they more effectively target tissue. The fields of polymer therapies and nanomedicines have seen enormous utilization of polymers<sup>(7)</sup>.

The goal of this work was to find a method to create a composite wound dressing using K-carrageenan and Na-alginate, In the presence of ZnO nanoparticles. The produced composite's efficacy as a dressing was assessed.

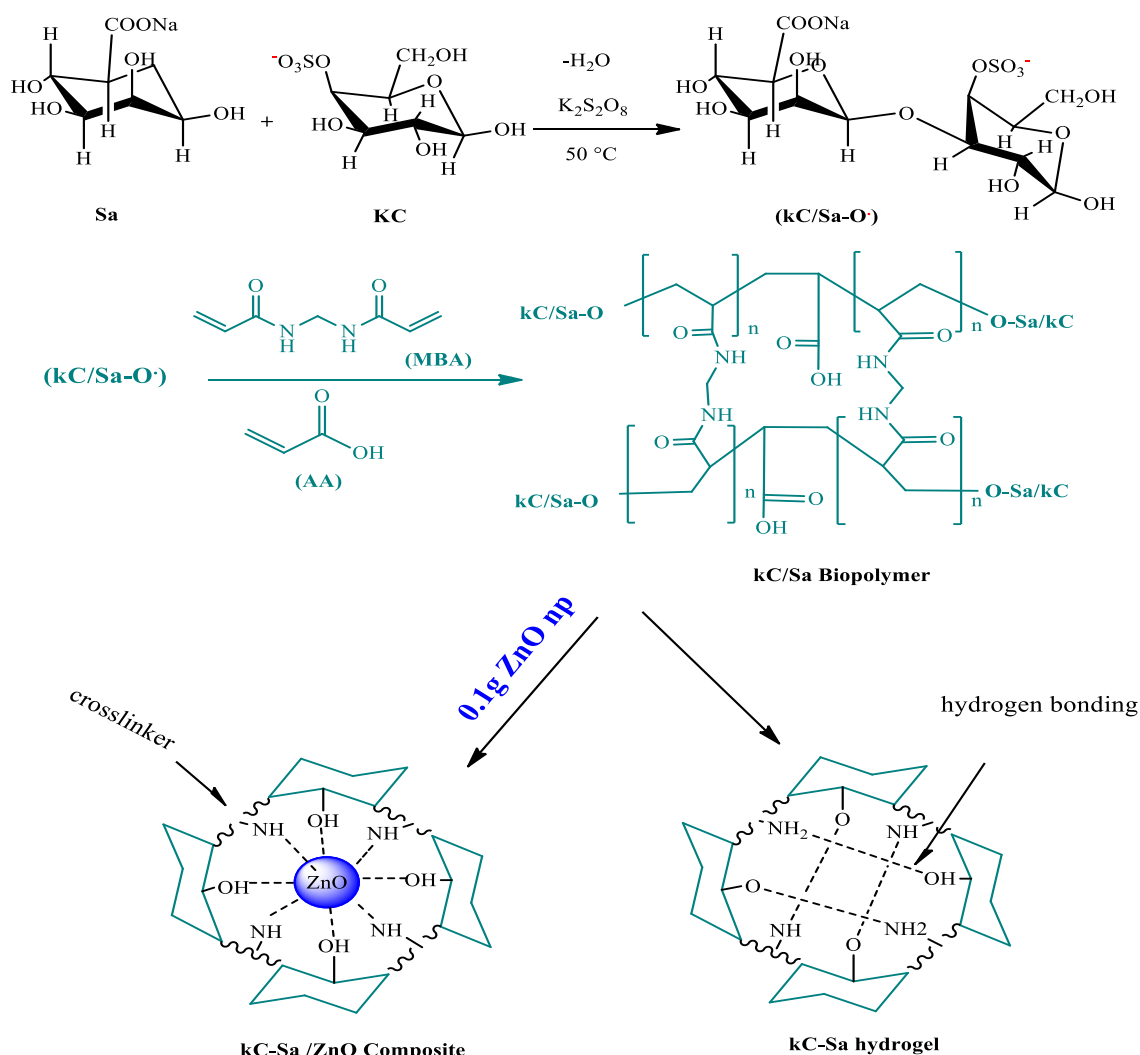
N,N'-methylenebisacrylamide (MBA), and acrylic acid (AA) (Chempur, Poland), and *Staphylococcus aureus* bacteria were obtained from Al-Diwaniya hospital (Al-Qadisiyah, Iraq) for type cultures. Mouse fibroblast cell line (L929) was obtained from the Iranian-type culture. Sprague Dawley rats aged 7 weeks were procured from Karbala University (College of Veterinary Medicine, Iraq) for wound healing tests. Double-distilled water (H<sub>2</sub>O), HCl, NaOH, and NaCl (94–97%) were used to study the drug release kinetics.

#### Preparation of hydrogel composites

The co-polymer of hydrogels was prepared by dissolving a 1:1 weight ratio of carrageenan and alginate in double-distilled water (H<sub>2</sub>O) while swirling vigorously until a vortex appeared to speed up the dissolution at a temperature of 60 to 65 °C to

#### Materials and Methods

Kappa carrageenan (KC), sodium alginate (Sa), hydroxychloroquine (HCQ), and diethyl ether were supplied by Sigma-Aldrich (Germany), potassium persulfate, zinc oxide nanoparticles, generate a homogeneous κC-Sa solution. To make κC-Sa/ZnO, ZnO NPs were solvated in 5 ml of acrylic acid (AA), and to make κC-Sa hydrogel, ZnO NPs were not used. The cross-linked N, N-Methylene-Bisacrylamide, and initiator potassium persulfate (K<sub>2</sub>S<sub>2</sub>O<sub>8</sub>) were added to the κC-Sa/ZnO solution after 25 minutes of continuous stirring. To finish the polymerization process, these solutions were placed in glass tubes and heated in a water bath. After that, bubbles are also removed using ultrasonography. The produced co-polymer was then dried in an oven at 65 °C after being washed with H<sub>2</sub>O. As seen in the finished form of the prepared polymer in Scheme. 1, the κC-Sa/ZnO hydrogel rocks were crushed into tiny pieces and sieved using a sieve with a mesh size of 150 mesh (Scheme. 1) (3,8,9).



Scheme 1. Synthesis of κC-Sa and κC-Sa/ZnO hydrogel composites

### Physical measurements

The hydrogel composites' cross-section and surface morphology were examined using a field emission scanning electron microscope (FE-SEM, EDX) with energy dispersive (Tescan, Czech, Iran) at a voltage of 25 kV. The Fourier transform infrared (FTIR) spectra of hydrogel and composite were monitored using an FTIR spectrometer (Shimadzu, Japan, 8400 s) ranging from 4000 to 400  $\text{cm}^{-1}$ . Since KBr allows light to pass through in the FT-IR measurement range, it is used as a carrier for the sample in the IR spectrum. Utilizing the hydrogels' cross-section and surface morphology and a TEM (transmission electron microscope) with 200 kV (Tescan, Czech, Iran).

### Swelling ratio

By immersing 0.1 g of the biopolymer sample in 100 mL of distilled water for eight hours with three repetitions. With the help of filter paper, the sample is separated from the water once it has been absorbed. The water acts as a solvent before it is weighed to estimate its mass. At 25°C, the swelling degree test is performed. The equation can be used to measure the magnitude of the degree of swelling.

$$Q = \frac{W_t - W_o}{W_o} \times 100\%$$

Q = swelling percentage of the hydrogel sample,  
W<sub>t</sub> = the weight of the sample after swelling, and  
W<sub>o</sub> = the weight of the sample before swelling

### Water evaporation rate

The prepared hydrogels were submerged in distilled water. After attaining swelling equilibrium, a specific weight of the hydrogel was taken, and it was then put for 24 hours at 50 °C in an incubator with a 50% humidity level. As the hydrogel dried completely, weight measurements were taken at regular intervals. The following equation <sup>(10)</sup> was used to get the water evaporation rate. (**Water lost percentage**) =  $(W_1 - W_2) / (W_1 - W_3) \times 100$  where W<sub>1</sub>, W<sub>2</sub>, and W<sub>3</sub> stand for the initial, measured, and final weights of the hydrogel, respectively.

### Antibacterial activity

The sensitivity test system was used in this study to examine the inhibitory biological effects of the compounds produced on one type of gram-positive bacteria by nutrient agar. The test bacteria are *Staphylococcus aureus*. The technique (Gram's Method) has also been used to make bacterial diagnoses. After 24 hours, the inhibitory zones of the bacteria were measured for width. By shaking 0.1 g of gel in a bacteria culture solution and placing it in a vibrator for two hours, it was then taken and cultivated using the agar diffusion method on a Petri dish<sup>(11)</sup>.

### In vivo wound healing

Three Sprague-Dawley male rats that were six weeks old were used to assess the hydrogel composites' ability to speed up the healing of wounds. All experiments were given ethical approval by the animal ethics committee at al Qadisiya University. For seven days, the test rats were acclimated in an animal facility with a relative humidity of 50% and a temperature of 25%. The test groups were separated into two groups at random: the first was treated as a control group without hydrogels, while the second was treated with hydrogel composites ( $\kappa\text{C-Sa}$  and  $\kappa\text{C-Sa/ZnO}$ ). In order to do the test, all mice were treated with a 0.1 g dose and rats were first given a 150-liter intraperitoneal injection of pentobarbital sodium. Their feet were then groomed, and a full-thickness (2-4 mm) acute wound was created on the side of the foot. Different hydrogels were applied to the excised wound at a rate of 0.1 g for each hydrogel, and a gel was put on the wound. On days 1, 7, and 14 of the experiment, excess diethyl ether was used to anesthetize rats. Incision wounds were carefully examined, and Image J software was used to estimate the degree of wound closure at 3, 7, and 14 days <sup>(12,13)</sup>.

### Histology

Rats were killed once on the 14th day of the test for histological findings. The skin was removed along with the surrounding healthy skin and treated overnight with 5% paraformaldehyde. Following the application of alcohol, the samples were embedded in paraffin, and cut into 4-5 mm cross sections using a microtome, and the skin healing and skin control were examined by histology <sup>(14)</sup>.

### Cytotoxicity assay

The cytotoxicity of  $\kappa\text{C-Sa}$  and  $\kappa\text{C-Sa/ZnO}$  against fibroblast cells was analyzed using the MTT assay. Tetrazolium salts are converted to insoluble formazan in the MTT experiment by the action of mitochondrial dehydrogenase enzymes in metabolically active cells as an indirect indicator of cell viability (a purple-colored compound). So, L929 fibroblast cells were seeded onto 24, 48, and 72 hour cell culture plates and incubated for 24, 48, and 72 hour in an incubator at 37 °C. Hydrogel samples were divided into small granules, after being sterilized for 30 minutes with 75% ethanol and used for 30 minutes under ultraviolet (UV) light, and each sample's absorbance was spectroscopically examined at 550 nm using a microplate reader<sup>(15)</sup>.

### Statistic

The SPSS 24 program (SPSS Inc., Chicago, USA) was used to perform the Pearson's correlation analysis. An analysis of variance one-way (ANOVA) was used to determine the statistical significance of the in vivo and in-vivo histology data at the 95% confidence level.  $P < 0.05$  was used to determine statistical significance, the mean SD is

used to express everything. When  $p < 0.05$ , differences were deemed significant<sup>(16)</sup>.

## Results and Discussion

The biopolymers prepared from algae, alginate (sodium alginate), and carrageenan (kappa carrageenan) have non-toxic biological properties associated with acrylic acid as a crosslinker, in addition to the use of zinc oxide nanoparticles as an additive to improve the properties of the polymer. The polymers were prepared by the free radical method using potassium persulfate ( $K_2S_2O_8$ ) in Scheme 1. The polymers were identified by FT-RT, FE-SEM, EDX, and TEM. The composite ( $\kappa$ C-Sa/ZnO) had higher properties than  $\kappa$ C-Sa in terms of swelling ratio, antibacterial activity, toxicity, and Wound healing.

## Characterization

### Fourier transform infrared spectroscopy

Figure. 1 and Table. 1 display the FTIR spectra of the pure hydrogel ( $\kappa$ C-Sa) and hydrogel composite ( $\kappa$ C-Sa/ZnO). The hydrogel was purified several times by dd-water to remove all suspended impurities and spectral contaminants until a spectral baseline of zero was verified for washing the hydrogels<sup>(17)</sup>. The hydroxyl group (OH) of alginate-carrageenan's stretching vibration caused all the hydrogels to exhibit a recognizable wide-stretching frequency at  $3100\text{--}3500\text{ cm}^{-1}$ . Alginate-carrageenan polymers with C-H alkane groups have a stretching vibration of  $2938\text{--}2952\text{ cm}^{-1}$ , while the SH bond<sup>(18)</sup> symmetric stretch has a peak at  $2667\text{--}2680\text{ cm}^{-1}$ . Peaks at  $1539\text{--}1542$  and  $1246\text{--}1250\text{ cm}^{-1}$ , and the usual amide and sulfate ester groups of alginates-carrageenan in both hydrogels, respectively, were identified as the sources of these signals, and there is no appreciable difference in the infrared regions because the interaction between the gel and the nanomaterial is a physical interaction. ZnONPs and cross-linkers were added; overall, the chemical structure of alginate-carrageenan did not alter significantly. However, the weak interactions between molecules of hydrogen alginate, carrageenan, ZnONPs, and crosslinkers resulted in a modest increase in the composite hydrogel's peak intensity. The spectra of prepared  $\kappa$ C-Sa hydrogel ( $\kappa$ C, Sa) observed the shift of (O-H) to a lower wavenumber due to the formation of new hydrogen bonding in ( $\kappa$ C-Sa) polymer, while ZnONPs increased the polarity in  $\kappa$ C-Sa/ZnO composite, which gave a higher wavelength at a higher absorption range<sup>(19-22)</sup> and the Zn-O bond appeared at around  $460\text{--}490\text{ cm}^{-1}$ <sup>(23,24)</sup>

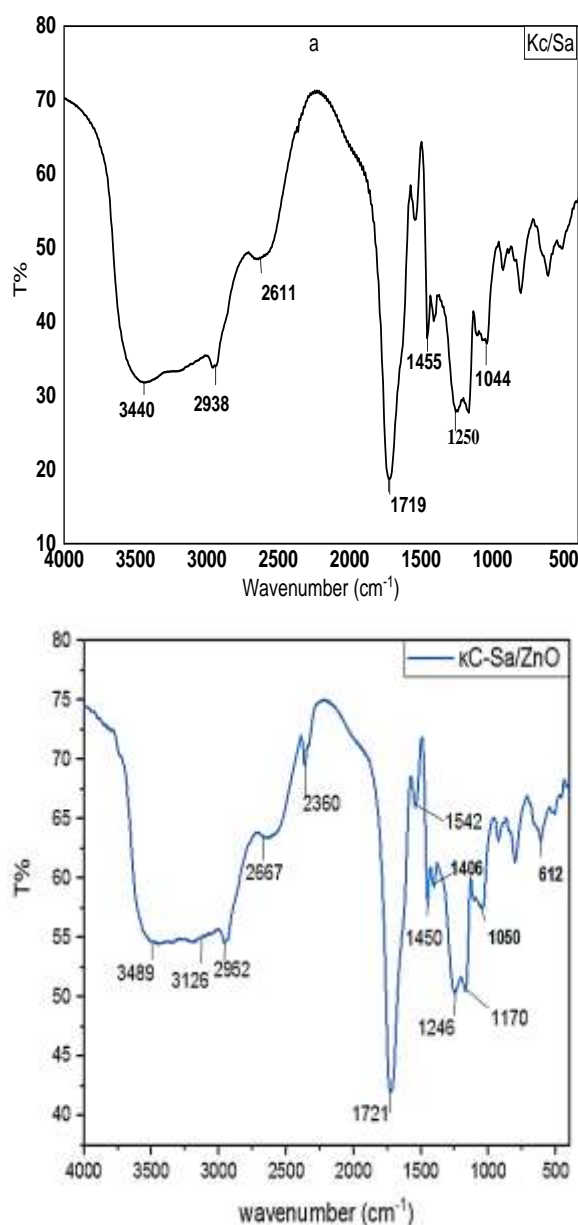


Figure 1. FT-IR spectra of  $\kappa$ C-Sa and  $\kappa$ C-Sa/ZnO hydrogels.



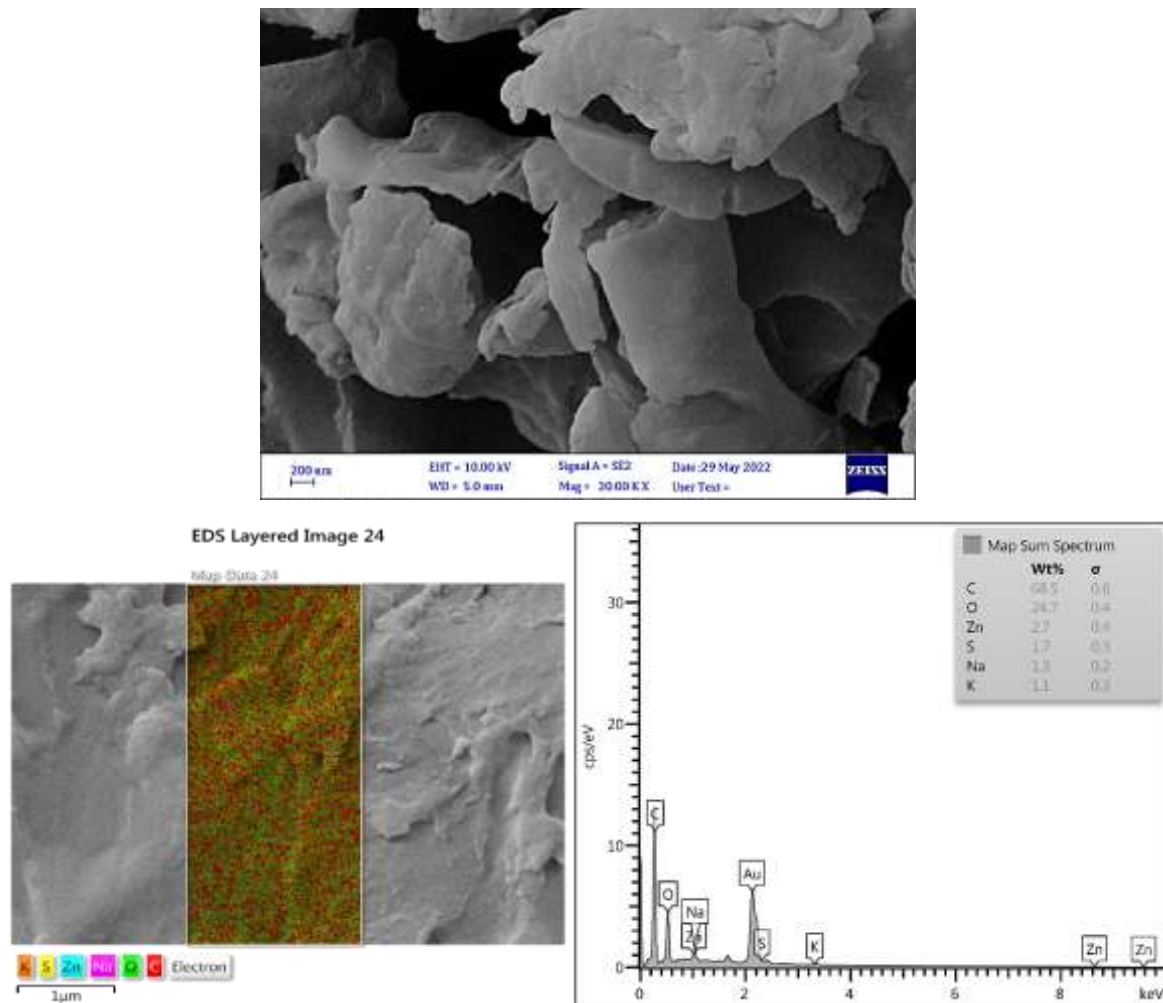


Figure 3. FE-SEM-EDX images and associated spectra of the  $\kappa$ C-Sa/ZnO composite at 200 nm.

#### Transmission electron microscopy (TEM) assessment:

As depicted in Figures. 4 and 5, the  $\kappa$ C-Sa and  $\kappa$ C-Sa/ZnO hydrogel composites were assessed with the help of transmission electron microscopy ("TEM"). The images of  $\kappa$ C-Sa shown in Figure. 4 were without zinc oxide particles, and the images

showed a uniform distribution of ZnO with a spherical shape and a randomly distributed layer in  $\kappa$ C-Sa/ZnO composite surface. The individual ZnO particles on the  $\kappa$ C-Sa/ZnO surface were distinct, as depicted in Figure. 5. The produced ZnO-NPs in the  $\kappa$ C-Sa/ZnO

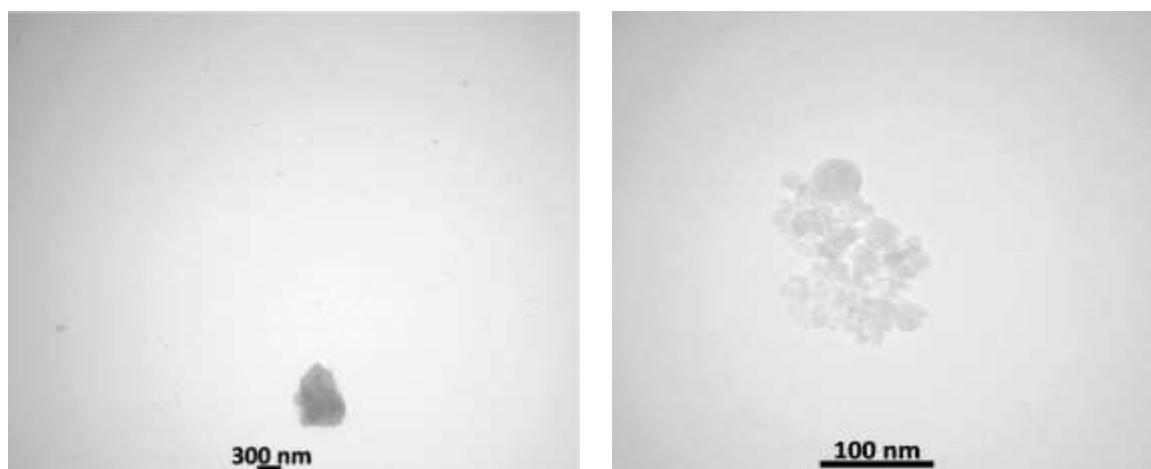


Figure 4. Transmission Electron Microscopy (TEM) photos of  $\kappa$ C-Sa hydrogel.

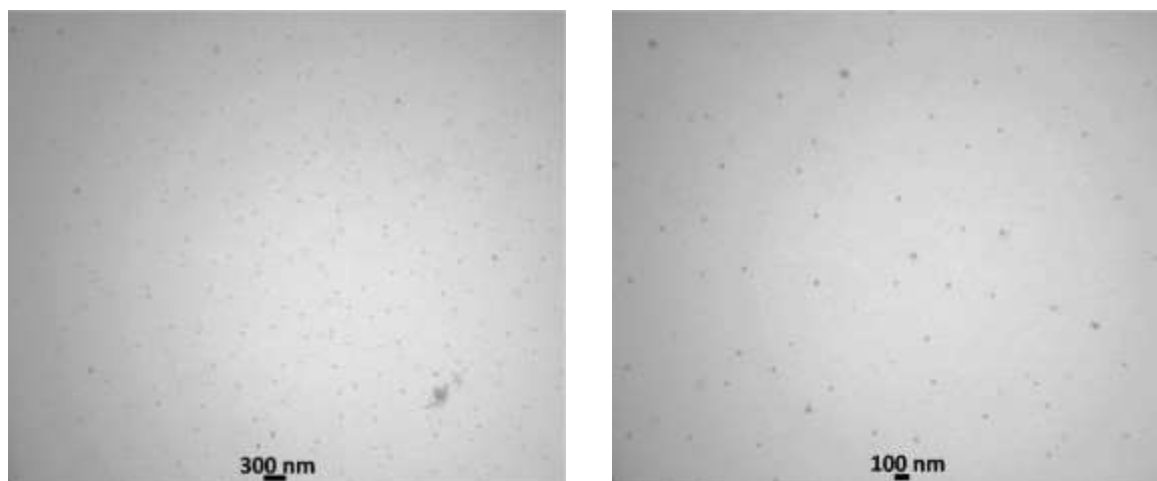


Figure 5. Transmission Electron Microscopy (TEM) photos of  $\kappa$ C-Sa/ZnO composite.

### Swelling ratio

It is ideal for the hydrogel's porous structure to have a high swelling ratio since this will help the wound site receive more oxygen, absorb wound exudates, and hold onto a lot of water. The swelling capacities of the  $\kappa$ C-Sa and  $\kappa$ C-Sa/ZnO hydrogels were evaluated by submersion in fluid for varying lengths of time; the repetition was done three times, and the average was taken in general (Figure. 6). With immersion time, all hydrogels' swelling ratios (SR) increased and stabilized after 6 hours. The addition of ZnONPs increased the swelling ratio, it is possible that the nanoparticles significantly enhanced the mechanical properties of the

nanocomposite hydrogel. The inclusion of ZnONPs boosted the nanocomposite hydrogel's swelling ratio, indicating that the nanoparticles significantly enhanced the hydrogel's mechanical properties, the  $\kappa$ C-Sa/ZnO hydrogel has 800% swelling<sup>(28)</sup>. Compared to the other hydrogel, as shown in Figure. 6. All nanocomposite hydrogels, including cross-linked ones, have a significant swelling ratio, which benefits the hydrogel's ability to absorb aqueous solution, such as AgNPs<sup>(29)</sup> and ZnONPs<sup>(25)</sup>. Additionally, 90% of the body's blood is water, and because hydrogels have great swelling properties, they can absorb a lot of the blood's water to help stop bleeding.

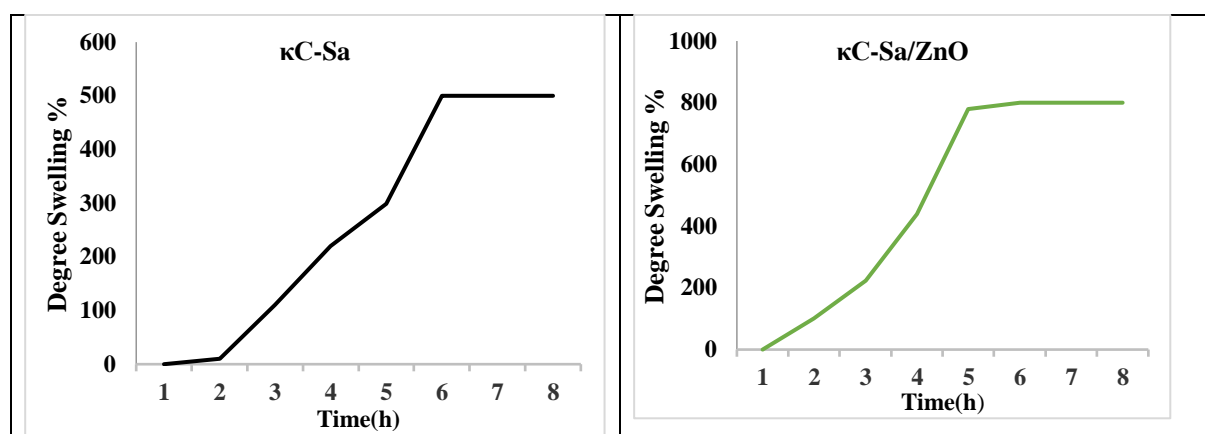
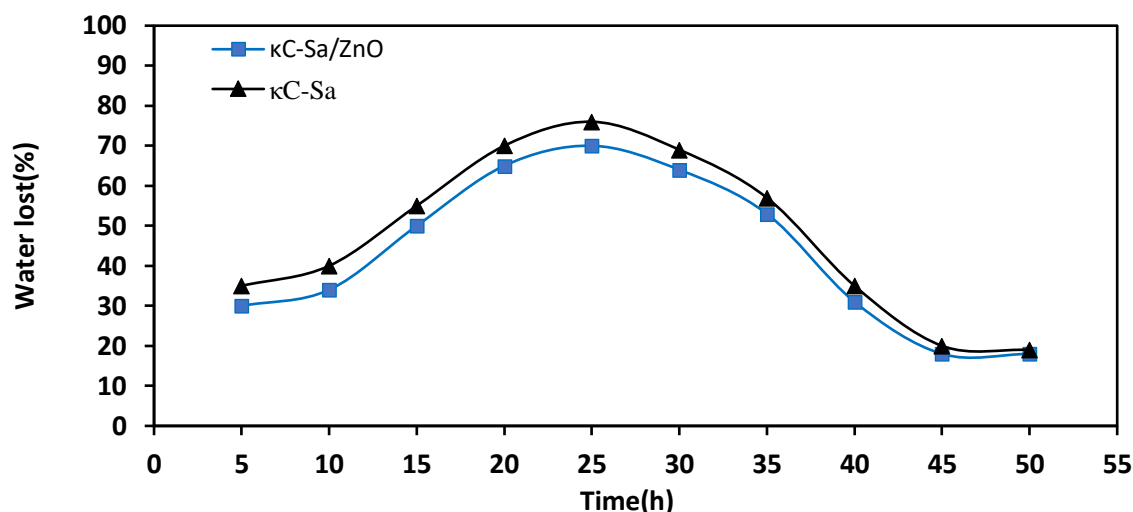


Figure 6. Swelling degree of  $\kappa$ C-Sa and  $\kappa$ C-Sa/ZnO composite.

### Water evaporation rate

The healing of the wounds can be accelerated in a moist environment. The best environment for efficient wound healing has long been recognized as one that keeps the wound bed moist. Water evaporation rate is another crucial characteristic of wound dressings, in addition to hydrogels' enhanced swelling properties. Before the wound heals in a clinic, replacement wound dressings must be applied repeatedly. Because the hydrogel dressings' water evaporation rate is lower, they need to be changed

less frequently, which leads to faster healing, less pain, and significant financial savings<sup>(30)</sup>. The percentage of water loss increased significantly between 30 and 75% during the course of ten hours, as seen in Figure 7. And it took 50 hours to obtain a steady swelling percentage. All of the hydrogels had retained 10%–20% of their original water after 50 hours. It demonstrates that the hydrogels have a high rate of water evaporation. In addition, it clung to the wound's surface to prevent blood vessels from rupturing<sup>(31,32)</sup>.



**Figure 7. Water loss of κC-Sa and κC-Sa/ZnO hydrogel prepare at different time in room temperature**  
*Antibacterial activity*

The antibacterial effectiveness of κC-Sa and κC-Sa/ZnO composite hydrogels was evaluated against gram-positive (*S. aureus*) bacteria, and the results are shown in Figure. 8. Alginate-carrageenan hydrogel (κC-Sa) and the control did not exhibit much antibacterial action against either bacterial strain, as was expected. In contrast, all alginate-carrageenan hydrogels combined with ZnONPs had

exceptional antibacterial activity against *S. aureus* the clear shapes theoretically. Sustained release of ZnONPs is one of the most desirable properties of hydrogels and their composites as wound dressing materials. The two hydrogels prepared have different biological properties, and that is very important as the translocation of germs into the wound will considerably alter the course of healing (33,34).

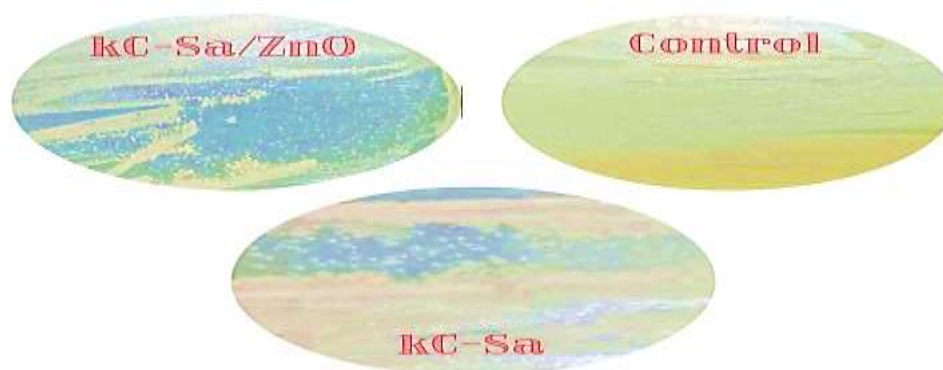


**Figure 8. Effect of hydrogels κC-Sa and κC-Sa/ZnO on staphylococcus bacteria**

#### *Cytotoxicity of hydrogels*

The proliferation of L929 cells was tested without tukey test to determine the biocompatibility of carrageenan-based hydrogels for 24, 48, and 72 hours. The results were displayed in Figure. 9. All test groups' cell densities were higher than the control's after 24 hours (more than 100%), indicating that no hydrogel composition was cytotoxic. Alginate/Carrageenan hydrogel and their composite were found to be biocompatible and not cytotoxic (35). The crosslinking agents used and the degree of crosslinking have a significant impact  $P \leq 0.05$  on the biocompatibility of the hydrogels. However,

after 48 hours of incubation, all test groups showed greater than 95% viability. Cell viability declined with incubation time (36). However, except for κC-Sa/ZnO hydrogel (94%), all hydrogel formulations dramatically reduced cell viability after 72 hours. The fast-growing L929 cells' lack of nourishment in the culture medium, which results in partial cell death, may be partly to blame for the decreased cell viability (29).so, indicating that these composites are good candidates for biomedical uses, This is because it is considered non-toxic when used as a wound adhesive and does not affect the environment or aqueous solutions.

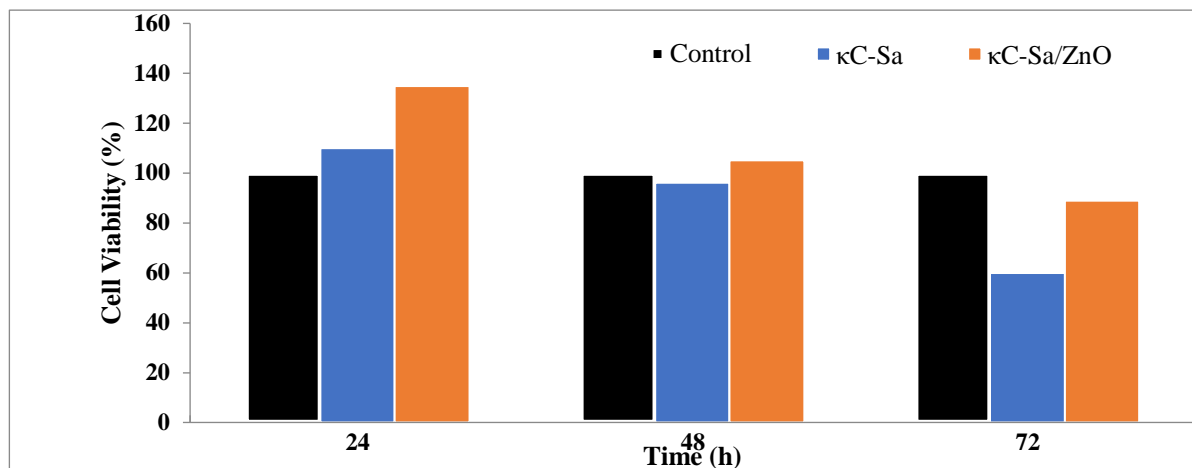


**Figure 9.** Cellular proliferation analysis of Control,  $\kappa$ C-Sa and  $\kappa$ C-Sa/ZnO hydrogels for the L929 (T-test of cells was used to calculate statistical significance (Benjamin-Hochberg p-values).not significant=  $P > 0.05$ ; Control ( $P \leq 0.05$ );  $\kappa$ C-Sa ( $P \leq 0.01$ );  $\kappa$ C-Sa/ZnO, ( $P \leq 0.0001$ ). The mean (SD) healing time for  $\kappa$ C-Sa/ZnO dressing was  $13.7 \pm 3.4$  while  $\kappa$ C-Sa hydrogel was  $15.6 \pm 3.7$ .

### Wound healing effect

Based on their functional characteristics, two types of hydrogels ( $\kappa$ C-Sa and  $\kappa$ C-Sa/ZnO composite hydrogels) were selected to test the hydrogels' ability to speed up the healing of wounds. Figure 10 illustrates the effects of composite hydrogels on the test rats' wound region and the apparent progress of wound healing. The dose for rats was 100 mg, and the dose was used in the form of a powder that was applied to the wound. Both outcomes demonstrated an apparent effect on wound healing (Figure. 10), and when full-thickness wounds on rats were photographed using a digital camera (Figure. 10), the rat's wound gradually shrank throughout the

course of treatment, on the other hand the kind of wound dressing substance has a substantial impact on how quickly the injury healed. 1, 3, and 14 days were spent receiving treatment, respectively. After 14 days of treatment with  $\kappa$ C-Sa and  $\kappa$ C-Sa/ZnO hydrogels, the fibro-proliferative tissue around the incision seemed to be fully healed. In contrast, after 14 days of hydrogel therapy, the  $\kappa$ C-Sa/ZnO hydrogel provided more healing than the  $\kappa$ C-Sa due to the combination of ZnONPs' superior antibacterial action and the  $\kappa$ C-Sa/ZnO hydrogel's outstanding wound healing effect. The mean (SD) by spss and healing time for  $\kappa$ C-Sa/ZnO dressing was  $13.7 \pm 3.4$  while  $\kappa$ C-Sa hydrogel was  $12.3 \pm 2.1$  <sup>(37,38)</sup>.

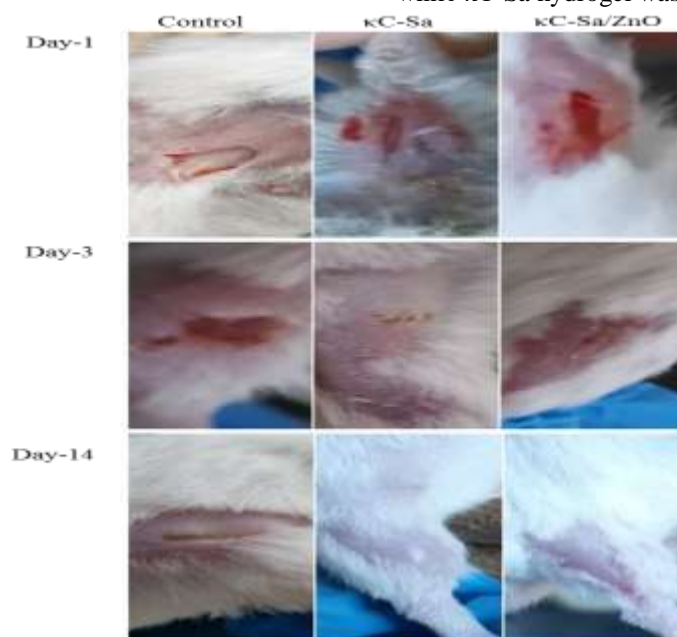


**Figure 10.** Evaluation of the healing of excisional foot skin wounds at 1, 7, and 14 days after the wound (dose: 100mg). The mean (SD) and healing time for  $\kappa$ C-Sa/ZnO dressing was  $13.7 \pm 3.4$  while  $\kappa$ C-Sa hydrogel was  $12.3 \pm 2.1$ .

### Histological analysis

To determine the degree of tissue healing, eosin-stained sections of the injury site treated with  $\kappa$ C-Sa and  $\kappa$ C-Sa/ZnO hydrogels underwent histological investigation. The results are displayed in Figure. 11. A, normal rat has collagen, hair, and hair follicles, as shown in Figure. 11B of the control group. Hyperplasia, an inflammatory infiltrate, glandular cavities, and many fibroblasts were all present after 14 days of therapy. The group that received  $\kappa$ C-Sa hydrogel treatment displayed a thick epidermis with glandular development, collagen fibers were swapped out for fibroblasts, and hair follicles, as shown by Figure. 11 C. By the way, the

skin healed to exhibit hair follicles, sebaceous glands, fibroblasts, collagen, and a thick epidermis with a distinct stratum corneum in the  $\kappa$ C-Sa/ZnO hydrogel treatment group's cell morphology, which was outstanding with complete epithelial regeneration. As a result, it can be said that the multifunctional composite hydrogels, particularly the  $\kappa$ C-Sa/ZnO hydrogel, exhibit outstanding wound healing effects and are biocompatible and antibacterial. The synergistic effect of  $\kappa$ C-Sa hydrogel and ZnO can be blamed for the faster healing effect in the treated groups than in the control group ( $\kappa$ C-Sa/ZnO)/ZnONPs<sup>(39-41)</sup>, as shown in Figure. 11 D.

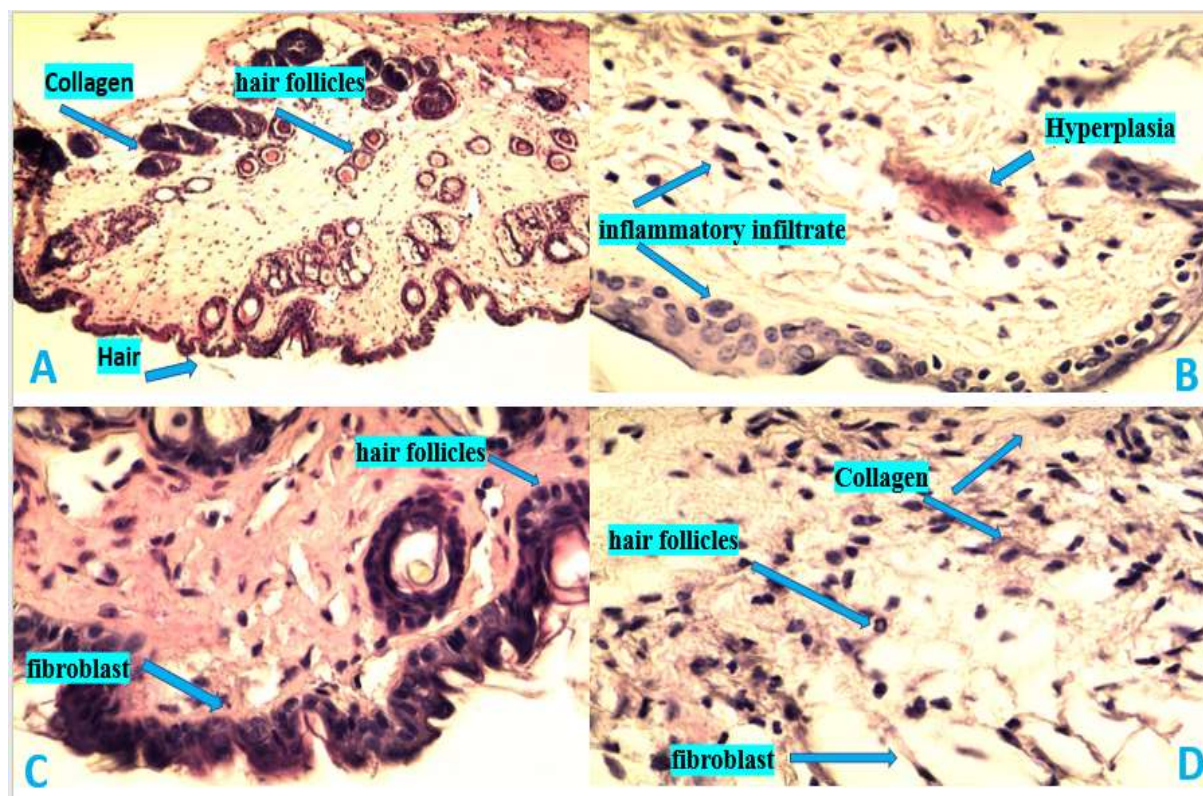


Figure 11. Histological appearance of wounded skin tissues: A. normal rat, B. control; C.  $\kappa$ C-Sa, D.  $\kappa$ C-Sa/ZnO, after 14 days of treatment.

### Conclusions

In the current study, we created alginate-carrageenan and its composites utilizing polysaccharides in a cost-effective and environmentally friendly manner. The produced hydrogel composites meet the requirements for being an optimal medication, according to the characterization experiments with SEM, EDX, TEM and FTIR. The two hydrogels,  $\kappa$ C-Sa and  $\kappa$ C-Sa/ZnO, were produced using a crosslinked synthesis of ZnONPs in an alginate-carrageenan matrix cross-linked with AA and MBA molecules. They are functional composite bio-hydrogels based on alginate and carrageenan. ZnONPs added to the polymer matrix increased the swelling ratio to the desired level while also providing antibacterial

activity. When used to treat full-thickness wounds in Sprague-Dawley rats, the hydrogels showed outstanding biocompatibility against dermal fibroblast cell lines (L929) and wound healing effectiveness.

### Acknowledgments

Acknowledgments and thanks to Dr. Layth S. Jasim Al-Hayder, for his encouragement and moral support during the scientific research.

### Conflicts of Interest

The authors declare that they have no known competing financial interests or personal relationships that could have appeared to influence the work reported in this paper.

## Funding

No specific grant was given to this research by funding organizations in the public, private, or not-for-profit sectors.

## Ethics Statements

The institutional ethical committee (University of Al-Qadisiyah, Veterinary Medicine College, Iraq) accepted the animal protocol to conduct the in-vivo wound healing activity and histological evaluation and were carried out in accordance with their requirements (Ref. No: 25-01-03-20-iraq).

## Author Contribution

A. F. G and M.K. A.; Writing-review & editing, L.S.J.: Supervision and Project administration, M.A.M.: Validation and all of the authors assessed the findings and gave their approval to the manuscript's final draft.

## References

1. Nezhad-Mokhtari P, Javanbakht S, Asadi N, et al. Recent advances in honey-based hydrogels for wound healing applications: Towards natural therapeutics. *J Drug Deliv Sci Technol.* 2021;66:102789. doi.org/ 10.1016/j.jddst. 2021. 102789.
2. Samarghandian S, Farkhondeh T, Samini F. Honey and health: A review of recent clinical research. *Pharmacognosy Res.* 2017;9(2):121. doi: 10. 4103/0974-8490.204647.
3. Al-Hussainawy MK, Al-Hayder LS.  $\kappa$ -Carrageenan/Sodium Alginate: A New Synthesis Route and Rapid Adsorbent for Hydroxychloroquine Drug. *Indones J Chem.* Published online 2023. doi.org /10. 22146 /ijc. 76819.
4. Zhang X, Li Y, He D, et al. An effective strategy for preparing macroporous and self-healing bioactive hydrogels for cell delivery and wound healing. *Chem Eng J.* 2021;425:130677. doi.org/10.1016/j.cej.2021.130677
5. Pereira DR, Silva-Correia J, Oliveira JM. RL. Reis, A. Pandit, MJ. Biggs, Nanocellulose reinforced gellan-gum hydrogels as potential biological substitutes for annulus fibrosus tissue regeneration. *Nanomedicine Nanotechnology, Biol Med.* 2018;14(3):897-908. doi.org/10.1016/j.nano.2017.11.011
6. Francesko A, Petkova P, Tzanov T. Hydrogel dressings for advanced wound management. *Curr Med Chem.* 2018;25(41):5782-5797. doi.org/10.2174/0929867324666170920161246\_2
7. Zaidi SA. Molecular imprinted polymers as drug delivery vehicles. *Drug Deliv.* 2016;23(7):2262-2271. doi.org/10.3109/10717544.2014.970297.
8. Kulal P, Badalamoole V. Hybrid nanocomposite of kappa-carrageenan and magnetite as adsorbent material for water purification. *Int J Biol Macromol.* 2020;165:542-553. doi.org/ 10.1016 /j.ijbiomac .2020.09.202.
9. Reghioua A, Barkat D, Jawad AH, et al, Magnetic chitosan-glutaraldehyde/zinc oxide/ Fe<sub>3</sub>O<sub>4</sub> nanocomposite: optimization and adsorptive mechanism of remazol brilliant blue R dye removal. *J Polym Environ.* 2021;29(12): 3932-3947.doi.org /10. 1007/ s10924 -021- 02160-z.
10. Zhou XB, Yang L, Wang GY, et al. Effect of deficit irrigation scheduling and planting pattern on leaf water status and radiation use efficiency of winter wheat. *J Agron Crop Sci.* 2021;207(3):437-449. doi. org/ 10.1111 /jac. 12466.
11. LSJ. Al-Hayder, M. Al-Hussainawy, A kinetics study of E. coli and S. aureus adsorption on cross linked hydro gels. *Int J ChemTech Res.* 2016;9(11):334-337.
12. Farshadzadeh Z, Pourhajibagher M, Taheri B, et al. Antimicrobial and anti-biofilm potencies of dermcidin-derived peptide DCD-1L against *Acinetobacter baumannii*: an in vivo wound healing model. *BMC Microbiol.* 2022;22(1):1-13. doi.org/10.1186/s12866-022-02439-8.
13. Crane MJ, Henry Jr, WL HL, Tran JE. Albina, Jamieson AM, Assessment of acute wound healing using the dorsal subcutaneous polyvinyl alcohol sponge implantation and excisional tail skin wound models. *JoVE (Journal Vis Exp.* 2020;(157):e60653. doi: 10.3791/60653.
14. Tayebi B, Babaahmadi M, Pakzad M, et al. Standard toxicity study of clinical-grade allogeneic human bone marrow-derived clonal mesenchymal stromal cells. *Stem Cell Res Ther.* 2022;13(1):1-18. doi.org/10.1186/s13287-022- 02899-9.
15. Pérez LA, Hernández R, Alonso JM, et al. Granular Disulfide-Crosslinked Hyaluronic Hydrogels: A Systematic Study of Reaction Conditions on Thiol Substitution and Injectability Parameters. *Polymers (Basel).* 2023;15(4):966. doi.org/ 10.3390 /polym1 50 40966.
16. Hu C, Chu C, Liu L, et al. Dissecting the microenvironment around biosynthetic scaffolds in murine skin wound healing. *Sci Adv.* 2021;7(22):eabf0787. DOI: 10.1126/ sciadv. abf0787.
17. Emwas AH, Saccenti E, Gao X, et al. Recommended strategies for spectral processing and post-processing of 1D <sup>1</sup>H-NMR data of biofluids with a particular focus on urine. *Metabolomics.* 2018;14:1-23. doi.org/ 10.1007 /s11306 -018-1321-4.
18. Zhu X, Su M, Tang S, et al Synthesis of thiolated chitosan and preparation nanoparticles with sodium alginate for ocular drug delivery. *Mol Vis.* 2012;18:1973.
19. Razali MH, Ismail NA, Yusoff M. Bio-Nanocomposite of Carrageenan Incorporating Titanium Dioxide Nanoparticles Scaffold and

- Hydrogel for Tissue Engineering Applications. *Nanoeng Biomater*. Published online 2022:295-321. doi.org/10.1002/9783527832095.ch27.
20. Jebur MH, Albdere EA, Al-Hussainawy MK, Alwan SH. Synthesis and characterization of new 1, 3-Oxazepine-4, 7-dione compounds from 1, 2-diaminobenzene. <https://doi.org/10.53730/ijhs.v6nS4.9123>.
  21. Moraes ANF, Silva LAD, de Oliveira MA, et al. Compatibility study of hydroxychloroquine sulfate with pharmaceutical excipients using thermal and nonthermal techniques for the development of hard capsules. *J Therm Anal Calorim*. 2020;140(5):2283-2292. doi.org/10.1007/s10973-019-08953-8.
  22. Waheeb AS, Alshamsi HAH, Al-Hussainawy MK, Saud HR. Myristica fragrans shells as potential low cost bio-adsorbent for the efficient removal of rose Bengal from aqueous solution: Characteristic and kinetic study. *Indones J Chem*. 2020;20(5):1152-1162. DOI: 10.22146/ijc.50330.
  23. Thangeeswari T, George AT, Kumar A. Optical properties and FTIR studies of cobalt doped ZnO nanoparticles by simple solution method. *Indian J Sci Technol*. 2016;9(1):4. DOI: 10.17485/ijst/2016/v9i1/85776.
  24. Aljeboree AM. Removal of vitamin B6 (Pyridoxine) antibiotics pharmaceuticals from aqueous systems by ZnO. *Int J Drug Deliv Technol*. 2019;9(2):125-9. doi: 10.25258/ijddt.9.2.3.
  25. Oun AA, Rhim JW. Carrageenan-based hydrogels and films: Effect of ZnO and CuO nanoparticles on the physical, mechanical, and antimicrobial properties. *Food Hydrocoll*. 2017;67:45-53. doi.org/10.1016/j.foodhyd.2016.12.040.
  26. Rhim JW, Wang LF. Preparation and characterization of carrageenan-based nanocomposite films reinforced with clay mineral and silver nanoparticles. *Appl Clay Sci*. 2014;97:174-181. doi.org/10.1016/j.clay.2014.05.025.
  27. Jaiswal L, Shankar S, Rhim JW, Hahm DH. Lignin-mediated green synthesis of AgNPs in carrageenan matrix for wound dressing applications. *Int J Biol Macromol*. 2020;159:859-869. doi.org/10.1016/j.ijbiomac.2020.05.145.
  28. Kyhoiesh HAK, Al-Hussainawy MK, Saud HR. Synthesis and characterization of polyacrylamide/crotonic acid and its composites with carbon nanotube and Rhodamine B. In: *AIP Conference Proceedings*. Vol 2398. AIP Publishing LLC; 2022:30018. doi.org/10.1063/5.0093386.
  29. Fan Z, Liu B, Wang J, et al. A novel wound dressing based on Ag/graphene polymer hydrogel: effectively kill bacteria and accelerate wound healing. *Adv Funct Mater*. 2014;24(25):3933-3943. doi.org/10.1002/adfm.201304202.
  30. JL. Gates, GA. Holloway, A comparison of wound environments. *Ostomy Wound Manage*. 1992;38(8):34-37.
  31. Yin H, Song P, Chen X, Huang Q, Huang H. A self-healing hydrogel based on oxidized microcrystalline cellulose and carboxymethyl chitosan as wound dressing material. *Int J Biol Macromol*. 2022;221:1606-1617. doi.org/10.1016/j.ijbiomac.2022.09.060.
  32. Liang Y, Bai Y, Xie AQ, et al. Solar-Initiated Frontal Polymerization of Photothermic Hydrogels with High Swelling Properties for Efficient Water Evaporation. *Sol RRL*. 2022;6(2):2100917. doi.org/10.1002/solr.202100917.
  33. Aa-S HK, Al-Hussainawy M. Spectral characterization and biological activity of 2-[2-(1-amino-1, 5-dinitrophenyl) azo]-imidazole, *J. Global Pharma Technol*. 2019;11(07):165-174.
  34. Kyhoiesh H, Al-Hussainawy MK, Waheeb AS, et al. Synthesis, spectral characterization, lethal dose (LD50) and acute toxicity studies of 1, 4-Bis (imidazolylazo) benzene (BIAB). *Heliyon*. 2021;7(9):e07969. doi:10.1016/j.heliyon.2021.e07969.
  35. Popa EG, Gomes ME, Reis RL, Cell delivery systems using alginate-carrageenan hydrogel beads and fibers for regenerative medicine applications. *Biomacromolecules*. 2011; 12(11):3952-3961. doi.org/10.1021/bm200965x.
  36. Pimton P, Ratphibun P, Tassaneesuwan N, et al. Cytotoxicity Evaluation of Hydrogel Sheet Dressings Fabricated by Gamma Irradiation: Extract and Semi-Direct Contact Tests. *Trends Sci*. 2022;19(13):4583. doi.org/10.48048/tis.2022.4583.
  37. Wang X, Ge J, Tredget EE, et al. The mouse excisional wound splinting model, including applications for stem cell transplantation. *Nat Protoc*. 2013;8(2):302-309. doi.org/10.1038/nprot.2013.002.
  38. Alavi M, Zorab MM, Ashengroph M, et al. Aljelehawy, D. Kahrizi, Antibacterial and wound healing applications of curcumin in micro and nano-scaffolds based on chitosan, cellulose, and collagen. *Cell Mol Biol*. 2022;68(3):9-14. DOI: 10.14715/cmb/2022.68.3.2.
  39. Jaiswal L, Shankar S, Rhim JW, Carrageenan-based functional hydrogel film reinforced with sulfur nanoparticles and grapefruit seed extract for wound healing application. *Carbohydr Polym*. 2019;224:115191. doi.org/10.1016/j.carbpol.2019.115191.
  40. Alkhursani SA, Ghobashy MM, Al-Gahtany SA, et al. Application of Nano-Inspired Scaffolds-Based Biopolymer Hydrogel for Bone and Periodontal Tissue Regeneration. *Polymers*

(Basel). 2022;14(18):3791. doi.org /10. 3390/  
polym 14183791.  
41. Enciso N, Avedillo L, Fermín ML, et al.

Cutaneous wound healing: canine allogeneic  
ASC therapy. Stem Cell Res Ther. 2020;11(1):1-  
14. doi.org/10.1186/s13287-020-01778-5.

## طريقة تخليق جديدة لمركبات البوليمر الحيوي المستندة على الالجنينات والكاراجينان و ZnONPS لتطبيقات التئام الجروح

علي فاهم قتران الخزعلي<sup>١</sup>، محمد قاسم الحسيناوي<sup>٢\*</sup>، مكارم علي مهدي<sup>٣</sup> وليد خالد عبد الصاحب<sup>٤</sup> و ليث سمير جاسم الحيدر<sup>٥</sup>

<sup>١</sup> قسم الكيمياء الصيدلانية، كلية الصيدلة، جامعة القادسية، الديوانية، العراق  
<sup>٢</sup> وزارة التربية والتعليم، مديرية تربية المثنى، السماوة، المثنى، العراق.  
<sup>٣</sup> قسم الكيمياء، كلية التربية، جامعة القادسية، الديوانية، العراق.  
<sup>٤</sup> قسم العقاقير والسموم، كلية الصيدلة، جامعة الفراهيدي، بغداد، العراق.  
<sup>٥</sup> الجامعة الوطنية للعلوم والتكنولوجيا، الناصرية، ذي قار، العراق.

### الخلاصة

تعتبر الهلاميات المائية نظامًا لتوصيل الأدوية ولها أهمية كبيرة خاصة للتطبيق الموضعي في علاج الجروح المفتوحة. إن خصائصها غير اللاصقة والاحتفاظ بالرطوبة وامتصاص الإفرازات تجعلها مثالية لتطبيقات التئام الجروح. باستخدام طريقة تخليق جديدة، تم تصنيع الهلاميات المائية الطبية الحيوية كاراجينان / الجينات (κC-Sa) والكاراجينان / الجينات /أكسيد الزنك (κC-Sa/ZnO) من خلال بلورة الجذور الحرة المعدلة مع حمض الأكريليك كمتشابك. تم تمييز الهلاميات المائية باستخدام صور FTIR و FE-SEM و EDX و TEM والصور الفوتوغرافية. تم استخدام κC-Sa / ZnO و κC-Sa كمعالجين للجروح للفئران المصابة. تحتوي الهلاميات المائية المصنعة على بنية مجهرية وخصائص شبه بلورية وتوزيع ZnO جيد لـ κC-Sa / ZnO، زادت ZnONPs المضافة إلى مترابك البوليمر نسبة التورم إلى ٨٠٠٪. بينما نسبة فقد الماء لـ κC-Sa تزيد بنسبة ٧٦٪ عن κC-Sa / ZnO (70٪) في ٢٥ ساعة عند درجة حرارة الغرفة. يُظهر مترابك هيدروجيل κC-Sa / ZnO نشاطاً للمضادات الحيوية أكثر من κC-Sa. كانت الهلاميات المائية متوافقة حيويًا عند تقييم تأثيرها السام للخلايا باستخدام خط الخلايا الليفية للفئران (L929)، حيث كانت κC-Sa / ZnO أكثر توافقًا حيويًا من κC-Sa. قدم هيدروجيل κC-Sa / ZnO شفاءً أكثر من κC-Sa في ١٤ يومًا، وتم تشخيص ذلك عن طريق التحليل النسيجي.

الكلمات المفتاحية: مضاد البكتريا، كاراجينان-الجينات، مترابك، السمية الخلوية، هلام مائي، تضميد الجروح، جسيمات اوكسيد الزنك النانوي.